Expression profiling identifies novel Hh/Gli-regulated genes in developing zebrafish embryos

Sadie A. Bergeron [a],[1], Luis A. Milla [b],[1], Rosario Villegas [b], Meng-Chieh Shen [a],
Shawn M. Burgess [c], Miguel L. Allende [b], Rolf O. Karlstrom [a],*, Verónica Palma [b],*

[a] Department of Biology, University of Massachusetts, Amherst, MA 01003–9297, USA
[b] Center for Genomics of the Cell and Department of Biology, Facultad de Ciencias, Universidad de Chile, Casilla 653, Santiago, Chile
[c] National Institutes of Health, National Human Genome Research Institute, Bethesda, MD 20892, USA

Abstract

The Hedgehog (Hh) signaling pathway plays critical instructional roles during embryonic development. Misregulation of Hh/Gli signaling is a major causative factor in human congenital disorders and in a variety of cancers. The zebrafish is a powerful genetic model for the study of Hh signaling during embryogenesis, as a large number of mutants that affect different components of the Hh/Gli signaling system have been identified. By performing global profiling of gene expression in different Hh/Gli gain- and loss-of-function scenarios we identified known (e.g., *ptc1* and *nkx2.2a*) and novel Hh-regulated genes that are differentially expressed in embryos with altered Hh/Gli signaling function. By uncovering changes in tissue-specific gene expression, we revealed new embryological processes that are influenced by Hh signaling. We thus provide a comprehensive survey of Hh/Gli-regulated genes during embryogenesis and we identify new Hh-regulated genes that may be targets of misregulation during tumorigenesis.
© 2007 Elsevier Inc. All rights reserved.

Hedgehog (Hh)/Gli-mediated cell–cell signaling plays diverse roles during embryonic development. Across many species, secreted Hh proteins provide critical instructional cues that induce and pattern a wide range of embryonic tissues. In humans, inappropriate Hh signaling results in diverse developmental defects and is implicated in the induction, maintenance, and/or metastasis of up to 25% of human brain tumors [1,2].

One key feature of the Hh pathway is the versatility of the signal. In the developing central nervous system (CNS), Sonic Hh (Shh), one of the three Hh proteins so far described in vertebrates, acts as a morphogen to regulate expression of a series of homeobox transcription factors that convey dorsal/ventral neural identity. In addition to this role in cell fate decisions, Shh signaling also modulates neural progenitor proliferation and survival in the developing neural tube [3] and regulates stem cell maintenance within the embryonic and adult dorsal brain [4,5]. Recent studies have also implicated Shh directly in axon guidance, suggesting that localized Hh signaling affects cellular behaviors independent of a transcriptional response [6,7]. Hh proteins act through the transmembrane proteins Patched (Ptc) and Smoothened (Smo) to trigger an intricate cytoplasmic transduction machinery, ending in the downstream activation of the Gli family of transcription factors. In vertebrates, at least three Gli proteins (Gli1, Gli2, and Gli3) that are homologous to the single *Drosophila Cubitus interruptus* (*Ci*) gene [8] have been described. Extensive research has focused on understanding how Hh signals, transduced by Smo, regulate the activity of the three Gli proteins and on how this signaling determines the magnitude and quality of the resultant Hh-dependent target gene induction [9,10]. Gli proteins are zinc finger transcription factors that respond to Hh signals and then

---

* Corresponding authors. V. Palma is to be contacted at fax: +1 56 2 271 2983.
R.O. Karlstrom, fax: +1 413 545 3243.
E-mail addresses: karlstrom@bio.umass.edu (R.O. Karlstrom),
vpalma@uchile.cl (V. Palma).
[1] These authors contributed equally to the work.

regulate the transcription of Hh target genes, either activating expression (Class II Hh-responsive genes such as *nkx2.2a* and *ptc1*) or repressing expression (Class I Hh-responsive genes such as *pax7* and *dbx2*) [11]. Gli1 acts primarily as an activator, while Gli2 and Gli3 can act both as activators and as repressors, like Ci. In mammals Gli2 appears to be the major activator of Hh signaling in the ventral nervous system, while in zebrafish Gli1 is the major activator and Gli2 plays both activator and repressor roles in different regions of the CNS [12]. The current model suggests that a combinatorial "code" of Gli repressor and activator functions guides Hh-mediated cell proliferation and differentiation in the vertebrate embryo.

Recent evidence provided by Cayuso and colleagues [3] shows that Shh-regulated patterning, proliferation, and survival of progenitors are separable activities in the developing spinal cord, suggesting that each of these cellular properties is an independently regulated response to Shh/Gli signaling. Thus, Shh signaling appears to directly coordinate the growth and patterning of the developing neural tube through Gli-mediated transcriptional regulation of discrete sets of target genes, including members of the homeodomain protein and basic helix-loop-helix (bHLH) families such as *nkx2.2a* and *foxA2* [3]. Since Hh signaling can influence multiple developmental processes, the genes that are activated or repressed in each circumstance vary with cellular context and developmental time, and Hh-mediated gene regulation is likely to require cell-type-specific cofactors. To date, a handful of genes whose transcription is regulated directly by Hh/Gli signaling have been described in both mammals and teleosts [11,13] and analyses of their promoter regions have led to the identification of a consensus Gli binding motif within their regulatory sequences [14,15]. These genes are known to regulate a variety of cellular processes including proliferation, metabolism, and apoptosis [16]. Considering the multitude of developmental processes that are regulated by Shh signaling, we hypothesize that there are far more Hh target genes than have been characterized to date that allow the reiterative deployment of the Shh pathway to elicit such diverse cellular responses. While the task of determining the repertoire of direct targets of transcription factors is still daunting, especially for organisms with complex genomes, microarray profiling of gene expression has emerged as a powerful approach for identifying regulatory networks of genes.

To uncover global changes in gene regulation in the embryo, appropriate gain- and loss-of-function scenarios are needed. Fortunately, large-scale genetic screens have identified a number of zebrafish mutations that affect embryonic development by disrupting different components of the Hh signaling cascade [17,18]. Among these are *slow-muscle omitted* (*smu*), which inactivates the Smoothened receptor and blocks all Hh signaling [19–21], and *detour* (*dtr*), which inactivates Gli1, the main Hh effector in zebrafish [12].

We used these mutants to globally characterize transcriptional changes that result from altered Hh/Gli signaling in the vertebrate embryo. Using a microarray approach, we compared the transcriptional profiles of wild-type embryos to those of *smu* (*smo*) and *dtr* (*gli1*) mutant embryos and to embryos with hyperactivated Hh signaling following *shh* mRNA injection.

This strategy has allowed us to (1) identify known genes that may be direct or indirect targets of Hh/Gli signaling and (2) uncover novel roles for Hh signaling in known developmental processes.

Results and discussion

Microarray analysis

Changes in the transcriptional profiles were analyzed by microarray using a set of oligonucleotides representing 34,647 transcripts. Table 1 gives an overview of the number of transcripts that showed positive and negative regulation by Hh, while Supplemental Table S1 contains the complete list of genes on the microarray chips and the observed regulation by Hh signaling. Some of these genes have been previously linked to Hh signaling, while others have no reported Hh regulation (Fig. 1A). We also detected many genes of unknown function that respond to Shh, characterized only as ESTs (Fig. 1B). A similar microarray study was recently published that also identified a large number of Hh-regulated genes [22]. In this previous study by Xu et al., injection of mRNA encoding a dominant negative form of protein kinase A was used to mimic Hh activation [22], while loss of Hh signaling was induced by cyclopamine treatments. In contrast, our study used *shh* mRNA injections to induce Hh signaling, and loss of Hh signaling was examined using known Hh pathway mutants, providing a more direct manipulation of Hh signaling. Of 37 Hh-regulated genes with putative Gli binding sites found by Xu et al. [22], 13 showed similar regulation by Hh in our microarray analysis, 3 showed opposite regulation, and 21 showed no significant regulation by Hh signaling. Similarly, 14 genes were verified for Hh regulation by Xu et al., and of these, 12 showed similar regulation in our study (see Supplemental Table S1). This comparison indicates that the two methods effectively identified an overlapping set of Hh-regulated genes. While discrepancies in the results may indicate inconsistencies in the microarray analysis, they may also point to real differences in regulation that are due to the different methods of manipulating Hh signaling.

We analyzed the expression of a subset of genes from three categories (known Hh target genes, known genes but unknown as Hh targets, and novel genes) using whole-mount in situ hybridization (ISH). Table 2 shows a summary of the genes analyzed in this paper, the data obtained for them in the

Table 1
Global data on identification of Hh-regulated genes by microarray analysis

Experiment	Up-regulated genes		Down-regulated genes	
	Total	% novel	Total	% novel
smu vs WT	245	81	376	83
dtr vs WT	367	84	455	81
shh injected vs WT	203	80	163	72

Gene expression was analyzed using microarrays representing a set of 34,647 transcripts. Genes showing a greater than twofold up- or down-regulation were tallied.
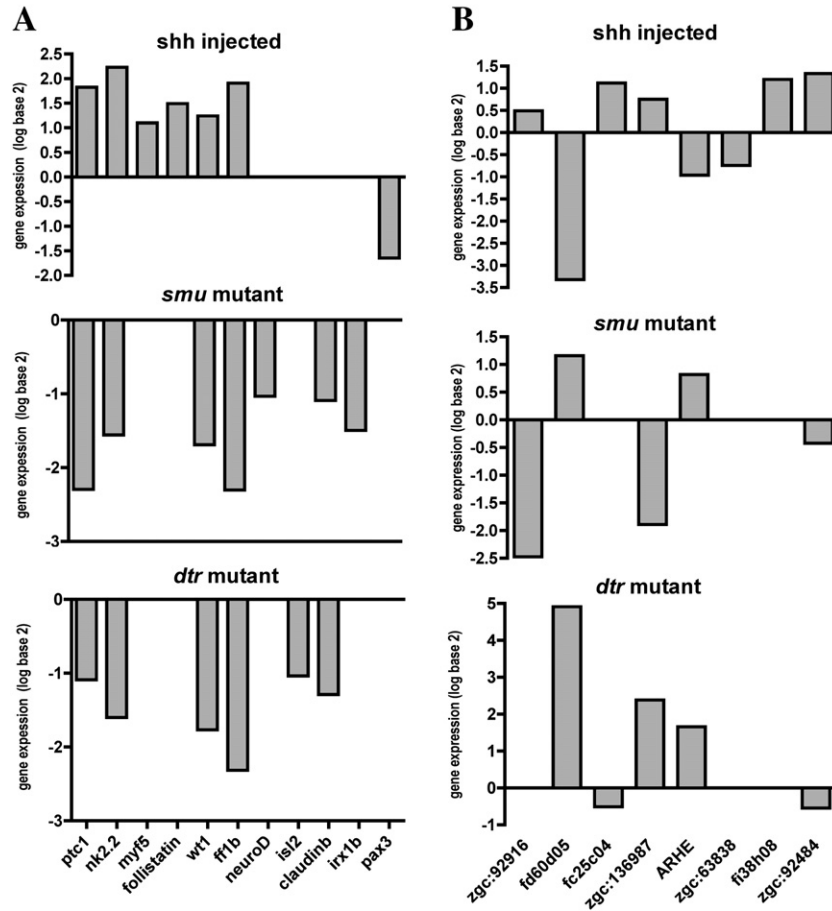
Fig. 1. Expression profiles of selected significantly up-regulated or down-regulated genes in embryos with altered Hh signaling. For each treatment, four replicate hybridizations were performed. The pattern of differential expression (median log 2 ratio) is graphically presented. (A) We chose 11 known genes and evaluated their expression profile in the different treatments. Among previously identified Shh-regulated direct targets, both *ptc1* and *nkx2.2a* are included and show the expected modulation. Also, 9 novel candidate Shh target genes were chosen based on their implication in cell growth and differentiation. These selected genes were independently confirmed as Shh target genes by whole-mount in situ hybridization. (B) We show 8 novel genes/ests that change their expression in the different treatments. Some of these genes were confirmed by in situ hybridization.

microarray assay, and whether regulation by Hh was verified by ISH. This microarray analysis could potentially identify direct transcriptional targets of Hh regulation as well as genes that were indirectly up- or down-regulated due to changes in tissue differentiation. To begin to identify which genes might be directly regulated by Hh, we scanned genomic sequences up to 5 kb upstream of the translational start site and 5 kb downstream of the translational stop for putative Gli transcription factor binding sites (GACCACCCA), as previously done by Xu et al. [22]. As shown in Table 2, 15 of 28 genes analyzed had at least two Gli binding sites in this region, suggesting they may be direct Hh/Gli transcriptional targets.

Verification of Hh regulation by whole-mount in situ hybridization

Changes in Hh signaling could affect overall gene expression levels in the embryo directly through changes in Gli-mediated transcriptional regulation (e.g., Class I and Class II Hh-responsive genes), indirectly through regulation of other transcription factors, or indirectly through global changes in the development of embryonic tissues [23]. To assess the relevance

of our data we thus decided to verify the gene regulation data obtained from the microarray using whole-mount ISH. In addition to allowing a relatively rapid verification of gene expression in different Hh-manipulated embryos, this approach provided spatial information and insights about the nature of regulation by Hh signaling. In the process, this approach also revealed new information about the role of Hh signaling in organogenesis. We immediately recognized several known Hh target genes among the genes showing regulated expression on the microarray. The well-characterized Hh receptor *ptc1*, as well as the early transcriptional target *nkx2.2a*, were appropriately regulated on the chip [24,25]. These data confirmed that our approach could identify direct Hh transcriptional targets. We next examined known developmental genes that were not previously reported to be regulated by Hh (e.g., Figs. 2–4). We also examined the expression of previously uncharacterized genes to determine whether gene expression differences seen on the microarray were reflected by differential expression in the embryo. Gene-specific primers based on published ESTs and genomic sequences (see Supplemental Table S1) were used to amplify coding regions from first strand cDNA, and antisense

Table 2
Summary of genes analyzed

	shh-inj/WT	smu/WT	dtr/WT	pGBS	Verified by ISH
Known Hh-regulated genes					
nkx2.2a[1]	4.7 (4.1)	0.3 (0.7)	0.3 (0.5)	1	+
patched1 (ptc1)[2]	3.5	0.2	0.5	12	+
olig2[3]	0.9	0.4	0.4	2	+
pax7[4]	0.6	1.7	0.6	12	+
Known genes (Hh reg. not defined)					
ff1b (nr5a1a)[5]	3.8	0.2	0.2	0	+
follistatin (fst)[6]	2.8 (2.0)	1.0 (0.6)	0.8 (1.0)	2	+
wilm's tumor (wt1a)[7]	2.4	0.3	0.3	n.d.	+
claudinb (cldnb)[8]	1.7 (1.3)	0.7 (0.5)	0.4 (0.6)	3	+
irx1b[9]	1.1	0.4	0.5	0	+
neuroD (nrd)[10]	0.9	0.5	1.0	0	+
pax3[11]	0.3 (0.6)	1.4 (1.6)	1.6 (0.8)	8	+
Novel genes/ESTs					
fv55h07 (zgc:63595)	28.4	0.0	0.5	3	−
fi60h10 (zgc:92484)	2.5	0.8	0.7	3	−
fr84a04 (zgc:85779)	2.4	0.9	0.5	n.d.	n.d.
fi38h08 (arhgef10)	2.3	1.6	0.6	7	+
EST: sim. SNF1-rel. kinase (zgc:73231)	2.2	0.3	0.4	2	−
fi41a08 (zgc:55473)	2.2	1.0	0.9	3	−
fd08b06 (fc25c04; follistatin-like 2 (fstl2))	2.2	0.9	0.6	1	+
fc21a11.x1 (GB Acc. No. AI641222)	2.1	0.0	0.0	1	n.d.
fo94g05 putative prot. of bilateral origin	1.9	0.7	0.6	1	−
fi31a01 DENN/MADD dom. prot.	1.8	1.0	1.0	n.d.	−
EST: (zgc:136987)	1.7	0.3	5.2	n.d.	+
fu20d03 zinc finger protein	1.5	0.4	10.1	1	−
EST: (zgc:92916)	1.4	0.2	1.2	1	+
EST: (zgc:63838)	1.3	1.7	0.8	6	+
fq35g11.x1 (GB Acc. No. BI710394)	1.2	0.0	0.0	1	n.d.
fm69b04.x1 (GB Acc. No. BI880051)	0.6	0.6	5.5	3	n.d.
EST: (arhe; sim. Mm. Rnd3a)	0.5	1.8	3.2	3	+
fb94e02 zinc finger protein 648	0.4	1.3	0.8	3	−
fb66a01 (zgc:153275)	0.4	0.8	0.9	n.d.	n.d.
fa08c02.s1 (GB Acc. No. AA542581)	0.4	1.0	10.7	1	n.d.
fl63b12 (smarca2)	0.3	0.6	0.9	14	+
fd60d05 solute carrier 6	0.2	2.2	30.5	n.d.	+

Values indicate fold change in gene expression seen on the microarray for each Hh manipulation, relative to wild type and uninjected controls. Numbers in parentheses show regulation of the same gene represented by an independent position on the chip. Dark green (increased expression) or red (decreased expression) shading indicates twofold change in expression, while lighter red or green shading indicates regulation slightly below this twofold cutoff. ISH, in situ hybridization; n.d., no data; pGBS, number of putative Gli binding sites; shh-inj., sonic hedgehog overexpression by mRNA injection. (For interpretation of the references to colour in this table legend, the reader is referred to the web version of this article.)
[1] NM_131422_1 (X85977), [2] X98883, [3] AF442964, [4] AF014370, [5] AF198086, [6] AF084948 (NM_131037_1), [7] NM_131046, [8] AF359426 (NM_131763), [9] AY017308, [10] AF036148, [11] NM_131277_1 (AF014366).

RNA probes were made directly from PCR-amplified products. Twenty two novel genes that showed regulation by microarray analysis were chosen for further analysis based on bioinformatic analysis suggesting they might play a role in embryogenesis. We were able to generate ISH probes for 16 of the 22 selected genes, and of these, 8 displayed appropriate regulation in mutant and/or shh mRNA-injected embryos.

Positively regulated known genes

follistatin (fst; GenBank Accession No. AF084948) and follistatin-like2 (fstl2; GenBank Accession No. A159257) regulation by Shh suggests a new regulatory mechanism for BMP signaling

Our microarray results indicated that *follistatin (fst)* expression was significantly up-regulated following *shh* mRNA injection (2.8× increase). Expression in *smu (smo)* mutants was reduced, but

at a level that just missed the twofold cutoff for significance on one of two microarray spots (0.6×). *fst* expression was relatively unchanged in *dtr (gli1)* mutant embryos (0.8×) (Table 2). An uncharacterized EST (fc25c04) related to *follistatin-like2* also showed positive regulation by Hh (2.2× in *shh* mRNA-injected embryos and 0.3× in *smu (smo)* mutants). *fst* is a well-known bone morphogenic protein (BMP) antagonist that is expressed in axial and paraxial mesoderm during late gastrula stages in zebrafish as well as later in the somites, brain, and eye [26]. *fst* was shown previously to inhibit a number of vertebrate BMPs including BMP2, BMP4, BMP5, and BMP7 [27,28]. Experiments in chick showed that *fst* can modulate the effects of BMP on Hh signaling, making neural progenitor cells more responsive to Hh signals and enhancing Hh-mediated differentiation into ventral cell types [29]. While it is known that a gradient of BMP signaling opposes the Hh signaling gradient in the neural tube, regulation of *fst* by Hh has not previously been demonstrated.
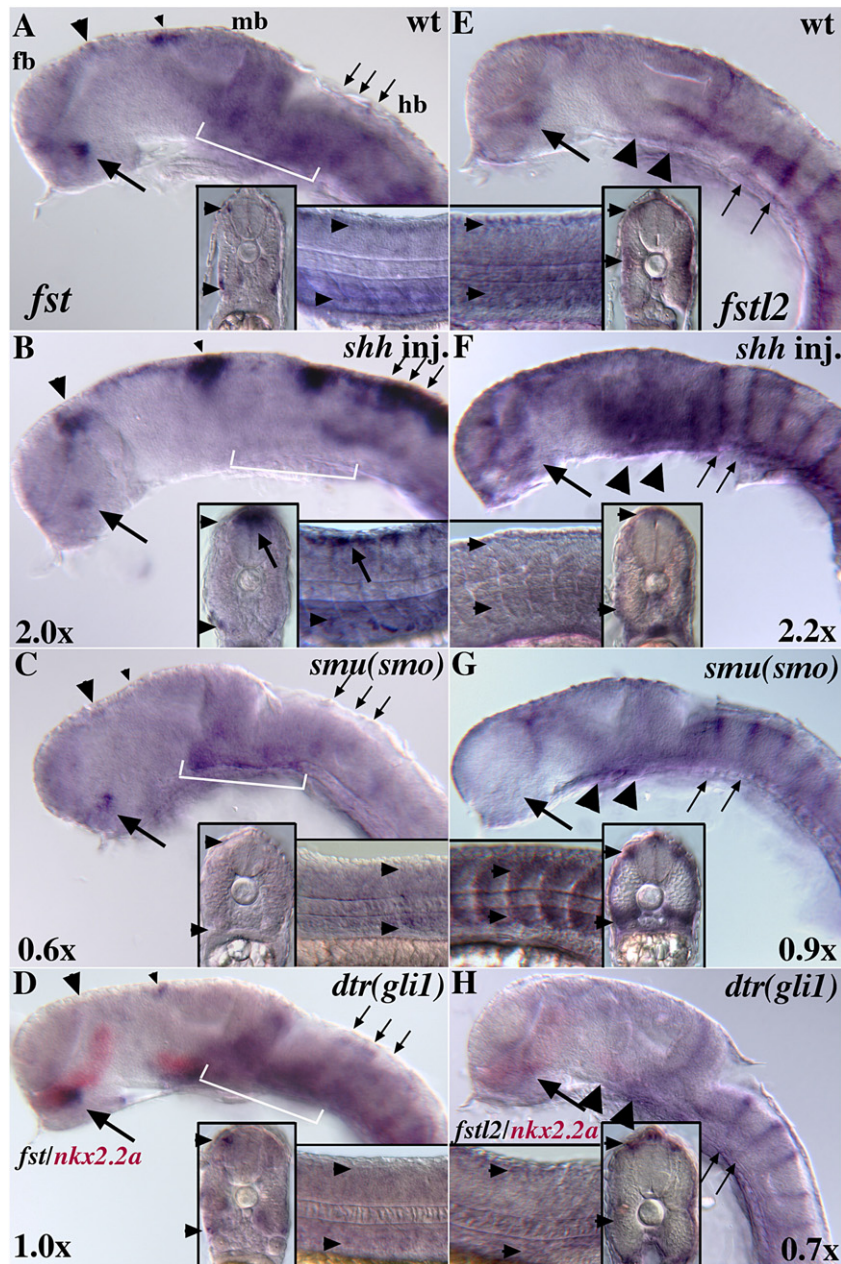
Fig. 2. Confirmation that *follistatin* (*fst*) and *follistatin-like2* (*fstl2*; *wu: fc25c04*) expression is affected by Hh signaling. (A) In wild-type embryos, *fst* is regionally expressed in the CNS, with weak dorsal expression in the region of the epiphysis (left arrowhead), tectum (right arrowhead), and hindbrain (thin arrows). *fst* is also expressed more ventrally in the diencephalon (arrow), midbrain, and hindbrain (white bracket). In the trunk, *fst* is expressed in ventral and dorsal regions of somites, but expression is undetectable in the dorsal spinal cord (insets, arrowheads). (B) In *shh* mRNA-injected embryos, dorsal *fst* expression is expanded in the diencephalon and midbrain (arrowheads), hindbrain (thin arrows), and spinal cord (insets, arrows). Ventral *fst* expression appears mildly reduced in the diencephalon (large arrow) and is reduced in the ventral midbrain and hindbrain (white bracket). (C) In *smu* (*smo*) mutant embryos, *fst* expression is lost in the dorsal brain (arrowheads) and reduced in the diencephalon (arrow), ventral midbrain, and hindbrain (white bracket) and somites (insets, arrowheads). (D) In *dtr* (*gli1*) mutant embryos, *fst* expression in the brain is similar to that in wild-type embryos, but may be slightly reduced in the somites (inset). Regional loss of *nkx2.2a* expression (red in D and H) confirms that this embryo is a homozygous *dtr* (*gli1*) mutant [12]. (E) *fstl2* is expressed in the ventral diencephalon (large arrow), in the ventral midbrain (arrowheads), and in stripes in the hindbrain that may correspond to rhombomere borders (small arrows). In the trunk *fstl2* is expressed dorsally and laterally in the somites (insets, arrowheads). (F) In *shh* mRNA-injected embryos, *fstl2* expression is regionally expanded in the ventral midbrain (arrowheads) but is mildly reduced in the somites (insets). (G) In *smu* (*smo*) mutants *fstl2* expression is regionally absent in the forebrain (arrow) and midbrain (arrowheads) but is expanded in the somites (insets). (H) In *dtr* (*gli1*) mutants CNS expression is reduced, while somite expression appears normal. Main panels show lateral views of 24-hpf zebrafish heads, eyes removed, anterior to the left. The corner insets show lateral views of the trunk, while the medial insets show cross sections through the trunk. In this and subsequent figures, the numbers in each panel indicate fold change in gene expression from microarray analyses. Fb, forebrain; mb, midbrain; hb, hindbrain.

ISH analysis confirmed that *fst* and *fstl2* expression was dramatically increased in the dorsal spinal cord and brain in *shh* mRNA-injected embryos (Fig. 2). *fst* expression was reduced in

the same dorsal regions in *smu* (*smo*) mutants and slightly reduced in *dtr* (*gli1*) mutants, consistent with positive regulation by Hh. The microarray analysis failed to uncover differential
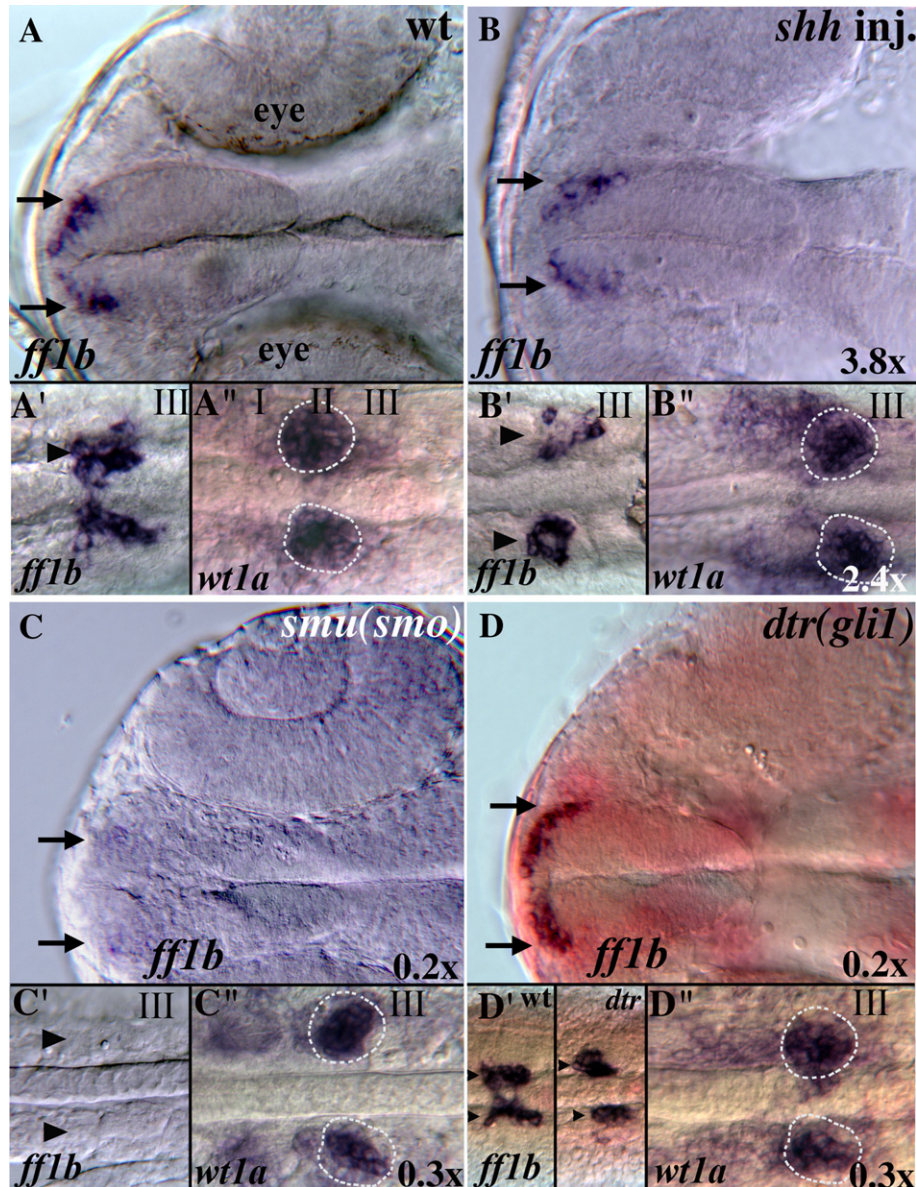
Fig. 3. Hh signaling affects *ff1b* and *wilms' tumor 1a* (*wt1a*) expression. (A–D) Ventral views of the heads of 24-hpf zebrafish embryos showing expression of *ff1b* in the optic stalk region of the forebrain (arrows). Forebrain *ff1b* expression is reduced in *shh* mRNA-injected (B) and *smu* (*smo*) mutant embryos (C) and appears slightly reduced in *dtr* (*gli1*) mutants (D). (A′–D′) Ventral views of the trunk between somites I and III showing *ff1b* expression in the interrenal gland primordia [66]. Additional *ff1b*-expressing cell clusters are present in *shh* mRNA-injected embryos (B′, arrowheads). Interrenal gland *ff1b* expression is absent in *smu* (*smo*) mutants (C′) and is slightly reduced in *dtr* (*gli1*) mutants (D′). (A″–D″) Ventral views of the trunk between somites I and III showing bilateral expression of *wt1a* in the developing pronephros [65]. *wt1a* expression is expanded in *shh* mRNA-injected embryos (B″ outside circle) and reduced in *smu* (*smo*) and *dtr* (*gli1*) mutants (C″ and D″, within circles). The circles represent the domain of wild-type *wt1a* expression.

expression of *fst* in *smu* (*smo*) mutants, most likely for technical reasons. *fstl2* was reduced ventrally and in the forebrain of *smu* (*smo*) mutants but increased elsewhere in the somites (Fig. 2), which may account for the almost unchanged overall expression detected on the microarray (0.9×). Regulation of *fst* expression by Hh could be direct, as the promoter region contains a putative Gli binding site (GA*A*CACCCA) that has a 1-bp difference compared to the Gli binding site found in the human *ptc1* promoter (GA*C*CACCCA) [22]. These results suggest that Hh signaling helps regulate expression of these BMP antagonists and may point to a new regulatory mechanism by

which antagonistic BMP and Shh signaling gradients are balanced to establish proper dorsal/ventral neural patterning.

ftz-f1 (*ff1b, nr5a1a;* GenBank Accession No. AF198086) and *wilms' tumor 1a* (*wt1a;* GenBank Accession No. X85734) regulation points to a role for Hh in interrenal gland and pronephros development

Our microarray data suggested that expression of the *ftz-f1* nuclear receptor homolog *ff1b* and of *wilms' tumor 1a* (*wt1a*) is highly influenced by Hh signaling. Both *ff1b* and *wt1a* are down-regulated in *smu* (*smo*) and *dtr* (*gli1*) mutants and up-

regulated in *shh* mRNA-injected embryos (*ff1b* 0.20×, 0.20×, and 3.75×; *wt1a* 0.26×, 0.29×, and 2.36×, respectively). *ff1b* is the apparent ortholog of mammalian SF1, an orphan nuclear hormone receptor transcription factor required for adrenal gland (interrenal gland in zebrafish [30]) organogenesis [31]. *wt1a* is a zinc finger transcription factor required for the proper formation of the vertebrate kidneys (pronephros in zebrafish) and the mammalian gonads [32]. It was previously shown that loss of *wt1a* function in zebrafish disrupts midline fusion of lateral pronephric cells and also results in a reduction in *ff1b* expression in the adjacent interrenal cells, suggesting a tight link between interrenal and pronephric development [33]. Therefore, diminished *ff1b* expression in Shh pathway mutants could be an indirect effect of the loss of *wt1a* expression. Hh signaling from the overlying notochord has also been implicated in pronephros and adrenal gland development [31,34], but regulation of these genes by Hh has not previously been demonstrated.

ISH analysis verified the changes in *ff1b* and *wt1a* expression levels seen by microarray (Fig. 3). In the trunk, interrenal gland expression of *ff1b* was absent in *smu* (*smo*) mutants (Fig. 3C′) and significantly reduced in *dtr* (*gli1*) mutants (Fig. 3D′), with apparently fewer cells expressing the gene. *ff1b* expression may be increased in *shh* mRNA-injected embryos because expression was expanded to as many as four distinct clusters of cells (Fig. 3B′). Similarly, *wt1a* expression in the pronephric primordia was significantly reduced in *smu* (*smo*) and *dtr* (*gli1*) mutants and was expanded in *shh* mRNA-injected embryos (Figs. 3B″, C″, and D″). *ff1b* expression was also reduced in the forebrain of *smu* (*smo*) and *dtr* (*gli1*) mutants (Figs. 3C, D). Interestingly, *shh* mRNA injection also reduced forebrain *ff1b* expression (Fig. 3B). The fact that both excess and reduced Hh signaling reduces expression of *ff1b* in the forebrain suggests that these *ff1b*-expressing cells may require an optimal, middle level of Hh signaling to differentiate. In *shh*-injected embryos, increased expression of *ff1b* in the trunk appears to overshadow this loss of forebrain expression to produce the overall increase in expression seen in the microarray experiments.

Despite the lack of *ff1b* in *smu* (*smo*) mutants (Fig. 3C), the interrenal primordia are able to form, as indicated by expression of the steroidogenic tissue marker *cyp11a1* (*scc*) in these mutants [33]. This suggests *ff1b* is not required for *scc* expression, as had been suggested by *ff1b* knockdown experiments in zebrafish [35]. Our ISH analyses suggest that Hh signaling plays an important role in interrenal and pronephric primordia development. This role for Hh appears to be evolutionarily conserved, as mice expressing a dominant-negative form of the Hh-responsive transcription factor *Gli3* do not develop adrenal glands [36]. Our data may help direct further investigations into the link between Hh signaling, interrenal *ff1b* expression, and pronephric *wt1a* expression during organogenesis of the adrenal gland and kidney.

iroquois 1b (irx1b; GenBank Accession No. AY017308): possible feedback between irx genes and the Hh pathway

Our microarray data showed a down−regulation of *irx1b* expression in both *smu* (*smo*) and *dtr* (*gli1*) mutants (0.36× and 0.5×, respectively). The *irx* genes are highly conserved homeodomain transcription factors that have been implicated in

the patterning of diverse tissues during development, such as the dorsal head and notum of *Drosophila* and the neural plate and heart in vertebrates (reviewed by Cavodeassi and colleagues [37]). Previously, regulation of *irx* genes by Hedgehog signaling has been shown in flies, chicks, and frogs. Patterning of the larval wing disc in *Drosophila* involves activation of *iro-C* complex genes by Hh/Ci signaling [38]. The *Xenopus Xiro1* gene is strongly activated in the anterior neural plate by overexpression of *Ci* [39]. In the chick as well as in the zebrafish, *irx3*, together with other homeodomain transcription factors, affects dorsoventral patterning of the neural tube [11]. *irx3* is a Class I gene, repressed by Shh, and its expression domain defines the region where V2 neurons will form in the ventral neural tube. Conversely, *irx1a* can regulate *Shh* itself, as seen in the developing zebrafish [40], suggesting a feedback loop between these genes. Whether the relationship between Hh signaling and the *iroquois* genes is direct or indirect remains to be determined.

irx1b expression in wild−type embryos is restricted to the CNS at 24 hours postfertilization (hpf), including the dorsal diencephalon and midbrain, hindbrain, cerebellum, lateral floor plate, and spinal cord (Fig. 4A, [41]). ISH analysis verified that *irx1b* is down-regulated in *smu* (*smo*) mutants, with expression regionally lost in the midbrain and generally reduced in the tail (Fig. 4C). *irx1b* expression was similarly reduced in *dtr* (*gli1*) mutant embryos (data not shown), consistent with the reduction seen on the microarray. While no overall change due to *shh* mRNA injection was seen on the microarray or by ISH, subtle regional changes in *irx1b* expression were detected in *shh*-injected embryos (Fig. 4B). Most notably, the expression domain encompassing the posterior diencephalon and anterior midbrain was expanded.

claudin b (cldnb; GenBank Accession No. NM_131763) indicates Shh modulation of genes in the otic placode

cldnb was significantly down-regulated in *smu* (*smo*) and *dtr* (*gli1*) mutant embryos (0.47× and 0.41×, respectively), with little change seen in *shh*-injected embryos. Claudins are members of the tetraspanin superfamily of integral membrane proteins specific to vertebrates that participate in cellular adhesion and migration and form vertebrate tight-junction strands [42] in various embryonic and adult structures [43]. In mammals, the family comprises at least 20 members, and genetic lesions in claudins are known to be the cause of defects such as kidney Mg^{2+} resorption [44] and deafness [45]. In zebrafish, *cldnb* is expressed in the developing ear and in lateral-line placodes, olfactory placodes, and pronephric duct and subsequently in the lateral line primordia, with *cldnb* being expressed strongly in the migrating primordia and in all neuromast accessory cells [46].

Our ISH analysis confirmed the down-regulation of *cldnb* in *smu* (*smo*) mutant embryos at 24 hpf, with expression completely absent (Fig. 4F). *cldnb* expression appeared normal in *dtr* (*gli*) mutants (data not shown). Consistent with the microarray results, *cldnb* expression levels in *shh*-injected embryos resembled those seen in wild-type embryos, despite the change in otic vesicle morphology (Fig. 4E). Since otic placode morphology appears normal in *smu* (*smo*) mutants (Fig. 4F), the loss of *cldnb* expression in these mutants may represent specific regulation by

Hh. This analysis is the first to suggest regulation of *cldnb* by Hh activity.

neuroD (nrd; GenBank Accession No. AF036148): a proneural gene regulated by Shh

Our microarray analysis showed a decrease in *nrd* expression in *smu (smo)* mutants (0.47×) and no significant changes in *shh*-injected embryos (0.89×). *nrd* is a bHLH transcription factor expressed during neurogenesis [47] that is also required for pancreatic morphogenesis in mice [48]. In 24-hpf zebrafish *nrd* is expressed in the dorsal forebrain and ventral midbrain/hindbrain, as well as in the pancreas, lateral line placodes, the facial epibranchial placode, and the octaval/statoacoustic ganglion precursors (Fig. 4G, [49]).

ISH analysis confirmed the microarray results, showing a regional loss in *nrd* expression in *smu (smo)* mutants and regional changes in *shh* mRNA-injected embryos. In particular, *nrd* expression was lost in *smu (smo)* mutants in the anterior/ventral hindbrain, as well as in the pancreas (Fig. 4I). In *shh* mRNA-injected embryos, *nrd* expression was expanded in the dorsal forebrain, as well as in the pancreas (Fig. 4H). This analysis uncovers Hh regulation of *nrd* expression in several regions of the embryo. We were unable to identify a Gli motif in the *nrd* promoter within 5 kb 5′ of the translation start site, possibly indicating that this regulation by Hh signaling is indirect.

Negatively regulated known gene: pax3 (GenBank Accession No. AF014366), a Class I Hh-regulated gene

Microarray analysis revealed that *pax3* transcription was significantly down-regulated in *shh* mRNA-injected embryos (0.554×) and somewhat up-regulated in *smu (smo)* mutants (1.6×), similar to the known Class I gene *pax7* (Table 2). There was no significant change in *pax3* expression in *dtr* (*gli1*) mutants (0.82×). *pax3* is part of a family of paired-box-containing transcription factors that are involved in multiple developmental processes including neural tube closure, muscle differentiation, and neural crest cell differentiation [50]. In zebrafish, *pax3* is expressed in the dermomyotome [51], dorsal diencephalon, and spinal cord [13]. Hh has been shown to repress *pax3* expression in the chick [52] and zebrafish [53] somite and more recently in the zebrafish neural tube [13].

ISH confirmed the negative regulation of *pax3* by Hh signaling seen in the microarray analysis (Fig. 5). In *shh* mRNA-injected embryos, *pax3* expression was strongly reduced and was restricted to the very dorsal regions of the neural tube. In the absence of Hh signaling (*smu (smo)* mutants) *pax3* expression was expanded into the ventral neural tube. Consistent with the microarray data, little or no change in *pax3* expression was seen in *dtr (gli1)* mutants. Since neural
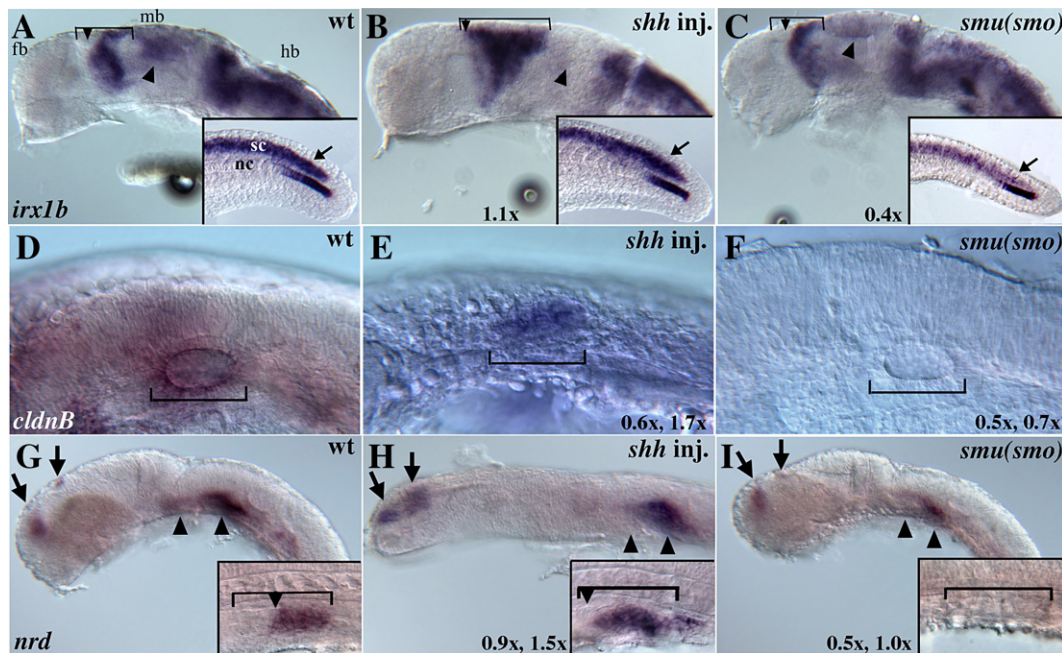

Fig. 4. *irx1b, claudinB,* and *neuroD* expression in embryos with altered Hh signaling. (A–C) Lateral views of 24-hpf embryos, eyes removed. (A) In wild-type embryos *irx1b* is expressed regionally in the midbrain, hindbrain, and spinal cord and in the caudal region of the notochord (inset) [67]. (B) In *shh* mRNA-injected embryos, *irx1b* expression is reduced in the tectum (arrowhead), but expression in the mid-diencephalon boundary is expanded caudally (brackets). *irx1b* expression is also slightly expanded in the caudal spinal cord (arrow in inset). (C) *irx1b* expression is reduced in *smu (smo)* mutants in the midbrain (arrowhead) and in the spinal cord (arrow in inset). (D) In wild-type embryos *claudinB* is expressed in the otic placode (bracket). (E) In *shh* mRNA-injected embryos this expression is expanded throughout the entire otic placode. (F) In *smu (smo)* mutants *claudinB* expression is completely absent. (G) In wild-type embryos, *neuroD* is expressed in the dorsal telencephalon and diencephalon of the forebrain (arrows), in the ventral hindbrain (arrowheads), and in the posterior half of the developing pancreas (inset). (H) In *shh* mRNA-injected embryos dorsal *neuroD* expression is expanded, and expression in the developing pancreas expands anteriorly (inset, bracket and arrowhead). (I) *neuroD* expression is extremely reduced in *smu (smo)* mutants, including in the developing pancreas (inset). Two numbers indicate regulation seen for genes represented by more than one oligo on the microarray chip.

cells are clearly present but fail to express *pax3* in *smu* (*smo*) mutants, these data suggest *pax3* is transcriptionally regulated by Hh signaling, either directly via Gli transcriptional regulation or indirectly via other Hh-regulated transcription factors. An analysis of the promoter region of *pax3* reveals Gli binding sites, suggesting Hh/Gli signaling may directly repress *pax3* expression, helping limit expression to the dorsal neural tube. These data help define *pax3* as a Class I Hh-regulated gene. Since *pax3* expression appears normal in *dtr* (*gli1*) mutants these data suggest that this Hh regulation of *pax3* may occur via Gli2 and/or Gli3 repressor activity.

Unknown gene regulated by Shh: novel Hh/Gli-regulated gene zgc:92916

Our microarray analysis identified over 300 putative Hh-regulated genes (Table 1). Many of these genes represent ESTs for which no function has been assigned. We chose to further examine several of these ESTs by ISH to determine whether they were indeed regulated by Hh signaling (Table 1) and to determine where in the embryo they are expressed as a first step toward a functional analysis. We present detailed data for one of these genes here.

Our microarray analysis showed that fr71a09.y1 (BI428994), which corresponds to the gene *zgc:92916* in zebrafish, was down-regulated in *smu* (*smo*) mutants (0.18×), and possibly up-regulated in *shh* mRNA-injected (1.4×) and relatively unchanged in *dtr* (*gli1*) mutant embryos (1.2×). zgc:92916 is 83% identical to mouse RAB3C and 90% identical to human Rab3C, a member of the Ras oncogene family of GTP-binding proteins that are involved in regulated endocytosis. Another member of this large protein family is Rab23, which has specifically been implicated as

a negative regulator in the Hh signaling pathway and is involved in trafficking of Smo in endosomes [54].

ISH analysis confirmed the microarray results. In 24-hpf wild-type embryos, *zgc:92916* is regionally expressed in the brain and spinal cord (Fig. 6A). In the brain, *zgc:92916* is expressed in the telencephalon, as well as in the anterior diencephalon, tegmentum, and ventral hindbrain, regions where Hh signaling is known to play an important patterning role. *zgc:92916* expression is regionally reduced in *smu* (*smo*) mutants, being mostly absent from the anterior diencephalon and tegmentum (Fig. 6C). In *shh* mRNA-injected embryos, *zgc:92916* is expanded dorsally in bands within the hindbrain (Fig. 6B), similar to the Hh-responsive gene *ptc1*. In the spinal cord *zgc:92916* is expressed in lateral columns of cells that may include differentiating motoneurons, interneurons, and commissural neurons. This expression is largely absent in *smu* (*smo*) (Fig. 6C) despite the fact that most of these neurons are present. Consistently, expression of *zgc:92916* in the lateral spinal cord appears increased in *shh* mRNA-injected embryos (Fig. 6B, inset).

Final remarks

Although it is clear that the endpoint in the Hh signaling transduction cascade is the regulation of diverse target genes, our present understanding of the number and kinds of genes regulated is limited. Shh can have multiple effects on adjacent cell types and distinct effects on the differentiation of a single cell type at different times. Under either scenario, the identification of transcriptional changes commanded by Hh that ultimately govern cell fate decisions is essential. Using a microarray-based approach, we investigated the molecular mechanisms by which Shh signaling modifies the transcriptional
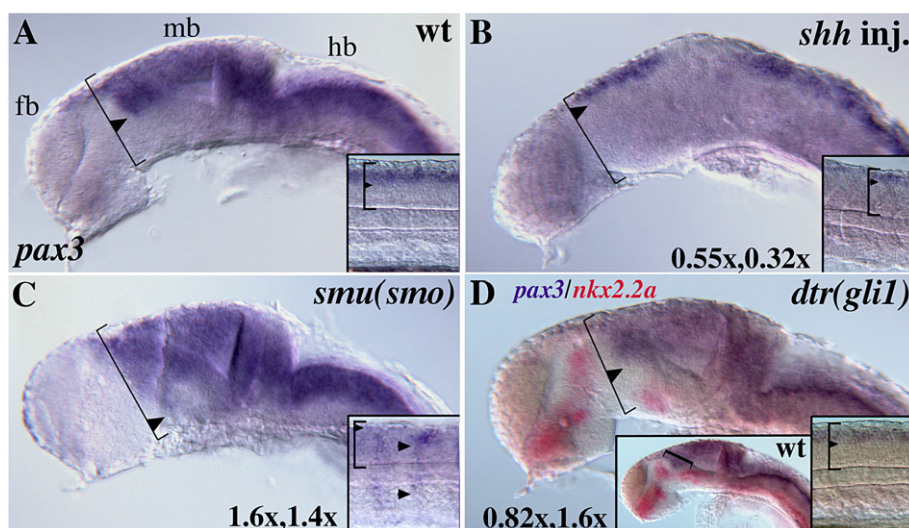

Fig. 5. *pax3* expression and Hh signaling. (A) In wild-type embryos, *pax3* is expressed in the dorsal spinal cord, hindbrain, and midbrain, with anterior expression stopping at the midbrain/forebrain boundary. *pax3* is also expressed in somites [64], but this expression is weak relative to CNS expression (inset). (B) In *shh* mRNA-injected embryos, *pax3* expression is greatly reduced in the CNS and is restricted to the dorsalmost region, while somite expression remains weak (inset). (C) In *smu* (*smo*) mutants, *pax3* expression is expanded ventrally in the midbrain (bracket, arrowhead). Somite expression of *pax3* is greatly increased in *smu* (*smo*) mutants (inset, arrowheads). (D) In *dtr* (*gli1*) mutants *pax3* expression appears normal in the brain and spinal cord (right inset). Regional loss of *nkx2.2a* expression (red labeling, bracket, compare to inset) confirms that this embryo is a homozygous *dtr* (*gli1*) mutant. Lateral views of 24-hpf embryos, eyes removed.

response of the early zebrafish embryo. We chose 24-hpf embryos, at which point the body plan has been laid out and Shh may function in roles other than patterning of the embryonic axes. Moreover, at this stage, *dtr (gli1)* mutants do not display significant tissue loss or necrosis, which could otherwise preclude the identification of bona fide target genes. This work complements a recent publication by Xu et al. [22], which described microarray-based expression profiling after global repression or activation of Shh signaling. Our study goes further since we took advantage of well-defined mutant loss-of-function conditions, and our zebrafish microarray contained twice the number of probes (34,647 versus 16,000). Moreover, we included the analysis of *dtr (gli1)* mutants in our experiments, aimed at dissecting the specific role of Gli1, the main effector of the pathway in teleosts. Further experiments will be needed to sort out whether regulation by Hh signaling is direct or indirect.

Studies of Shh function in a number of organisms have shown that the same signal can govern cell proliferation, survival, and fate, alternatives that must be context- and time-dependent. Given the remarkable network of gene activity regulated by Shh, this growth factor could function to ensure that independent mechanisms act on the correct number of precursors that can then respond to appropriate patterning signals in diverse structures. The classes of genes identified in this study correlate well with the possible outcomes of Shh activity. Genes implicated in cell proliferation, survival, and differentiation were activated by enhanced signaling, and they corresponded to a wide variety of cellular processes and molecular functions (Supplemental Fig. 1).

Our findings support a critical role for Shh in building the nervous system, confirming the current view that beyond its classical role in ventral patterning, brain growth is controlled by the mitogenic action of Shh at later embryonic time points. How the levels and duration of the Hh signal are integrated/modulated by the recipient cells depends also on how Hh signaling interacts with other signaling cascades, and several recent studies have begun to explore such a mechanism at the cellular level [55–57]. A major challenge in the field is to unravel the complex network of signaling interactions and to identify common targets susceptible to regulation by more than one inductive signal, as has been described for the EGFR [57] and β-catenin [55], key components of the EGF and canonical Wnt signaling pathways, respectively.

It is now clear that embryonic cell–cell signaling systems involved in cellular patterning play critical roles in tissue homeostasis, growth, and cancer [4]. In this sense, tumors can be seen as abnormal organ development processes that, nevertheless, display consistent order, morphogenesis, and patterning [58]. Our study contributes to the understanding of the role of the Shh pathway by highlighting some new genes that could be used as targets for drug development for rational anti-cancer therapies.

Materials and methods

Zebrafish lines

Wild-type and mutant zebrafish embryos were maintained at 28 °C as described in [59] and staged according to [60]. Mutant lines used were *smooth muscle omitted* (*smu*[hi1640]), a loss-of-function *smoothened* allele [19], and *detour* (*dtr*[ts269]), a loss-
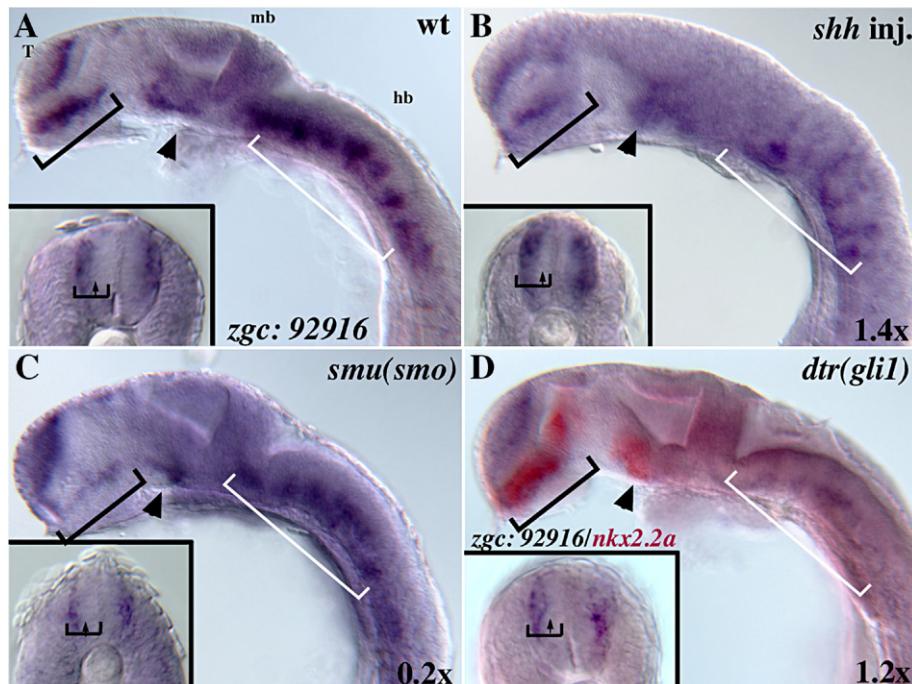

Fig. 6. Expression of novel gene *zgc:92916* and confirmation of its regulation by Hedgehog signaling. (A) In wild-type embryos, *zgc:92916* is expressed in the telencephalon (T), ventral hindbrain (white bracket), anterior/dorsal diencephalon (black bracket), and ventral midbrain (arrowhead) and bilaterally along the dorsal–ventral axis of the spinal cord (insets; A–D). (B) In *shh* mRNA-injected embryos this expression is expanded medially in the spinal cord (inset) and dorsally in the midbrain, and hindbrain. (C) In *smu* (*smo*) mutants *zgc:92916* expression is reduced in the anterior/dorsal diencephalon (black bracket), ventral midbrain (arrowhead), and spinal cord (inset). (D) The expression of *zgc:92916* in *dtr* (*gli1*) mutants was similar to that seen in wild-type embryos. The embryo in (D) was double labeled to show *nkx2.2a* expression (red) allowing unambiguous identification as a homozygous *dtr* mutant.

of-function *gli1* allele [12]. Mutants were maintained as heterozygotes and heterozygous adults were crossed to produce homozygous mutant offspring. Homozygous mutant individuals were identified by morphological criteria (curled body axes) and/or defects in *nkx2.2a* expression (*dtr*).

mRNA injections

shh mRNA was synthesized with T7 polymerase from the *shh*/T7TS plasmid [61] linearized with BamHI using the mMessage mMachine kit (Ambion). Wild-type embryos were injected with ~100 pg of *shh* mRNA at the one- to two-cell stage. Injected embryos were incubated at 28 °C until 24 hpf and fixed for in situ hybridization.

Embryo samples and RNA extraction

Total RNA was isolated from 100 embryos per experimental condition by placing the embryos in 1 ml Trizol reagent (Invitrogen) in an Eppendorf tube. Embryos were disrupted by grinding them using pestle tips or by vortexing for 1 min, with 500 mg of glass beads (Sigma), until embryos were clearly disrupted and then allowing the beads to settle before removing the supernatant. RNA was further purified using Qiagen Mini-RNA purification columns by resuspending the RNA in 50 μl of DEPC-treated H_2O and following the manufacturer's instructions for RNA cleanup.

Microarray analysis

The detailed protocol and normalization procedures were as in [62] and are available upon request. In brief, first-strand cDNA probes were generated by incorporation of aminoallyl dUTP and then coupled to the desired fluorochrome (Cy3 or Cy5). The resulting cDNA probes were purified and concentrated. All samples were hybridized to the arrays compared to a "reference" RNA sample (which consisted of embryos pooled from multiple stages of development) and changes of expression level were determined by comparing the signal intensity changes compared to the stable reference signal. Each chip contained 34,647 printed oligo elements (Compugen, Operon, and MWG) designed from zebrafish EST assemblies and representing approximately 20,000 genes, which represented approximately 60% of the total predicted genes according to the public Ensembl database. After hybridization, the slides were washed, dried, and scanned using an Agilent DNA microarray scanner (Agilent Technologies) at 635 nm (Cy5) and then at 532 nm (Cy3). Fluorescence intensities were quantified using Agilent feature extraction software (Agilent Technologies). To ensure that all data were directly comparable, we did two color hybridizations with one of the colors labeling a reference sample that was the same for all slides. This normalized any chip-to-chip variability by allowing us to take the "ratio of the ratios" in any given comparison. Hybridizations were performed twice, switching the fluorescent labeling to eliminate biases caused by the labeling process. Samples were normalized using the Lowess calculations (see Supplemental Fig. 1 for description) and cutoffs for significance were set at a twofold change in either direction. Oligo sequences were mapped to multiple databases, including RefSeq, UniGene, Ensembl, and TIGR, and genomic coordinates to maximally determine gene identity and function. Data were deposited into searchable FilemakerPro and Excel databases for analysis.

Whole-mount in situ hybridization

Whole-mount ISH at 24 hpf was performed as described [63], using digoxigenin-labeled probes (Roche). Embryos were postfixed in 4% paraformaldehyde overnight, cleared in 75% glycerol, and photographed using DIC optics on a Zeiss Axioskop. Available probes included *cldnb* [46], *irx1b* [41], *fst* [26], *nrd* [47], *pax3* [64], and *wt1a* [65]. In situ probes to novel genes were made using PCR-generated DNA fragments that contained the T7 (antisense primer) or SP6 (sense primer) RNA polymerase binding sites. PCR fragments were amplified from first-strand wild-type cDNA primed with oligo(dT) or random hexamer primers (Invitrogen cDNA Kit). Gene-specific primer sequences are listed in Table S1.

Appendix A. Supplementary data

Supplementary data associated with this article can be found, in the online version, at doi:10.1016/j.ygeno.2007.09.001.

References

[1] L. Lum, P.A. Beachy, The Hedgehog response network: sensors, switches, and routers, Science 304 (2004) 1755–1759.

[2] P.S. Knoepfler, A.M. Kenney, Neural precursor cycling at sonic speed: N-Myc pedals, GSK-3 brakes, Cell Cycle 5 (2006) 47–52.

[3] J. Cayuso, F. Ulloa, B. Cox, J. Briscoe, E. Marti, The Sonic hedgehog pathway independently controls the patterning, proliferation and survival of neuroepithelial cells by regulating Gli activity, Development 133 (2006) 517–528.

[4] M. Fuccillo, A.L. Joyner, G. Fishell, Morphogen to mitogen: the multiple roles of hedgehog signalling in vertebrate neural development, Nat. Rev., Neurosci. 7 (2006) 772–783.

[5] V. Palma, D.A. Lim, N. Dahmane, P. Sanchez, T.C. Brionne, C.D. Herzberg, Y. Gitton, A. Carleton, A. Alvarez-Buylla, A.R. Altaba, Sonic hedgehog controls stem cell behavior in the postnatal and adult brain, Development 132 (2005) 335–344.

[6] D. Bourikas, V. Pekarik, T. Baeriswyl, A. Grunditz, R. Sadhu, M. Nardo, E.T. Stoeckli, Sonic hedgehog guides commissural axons along the longitudinal axis of the spinal cord, Nat. Neurosci. 8 (2005) 297–304.

[7] F. Charron, E. Stein, J. Jeong, A.P. McMahon, M. Tessier-Lavigne, The morphogen sonic hedgehog is an axonal chemoattractant that collaborates with netrin-1 in midline axon guidance, Cell 113 (2003) 11–23.

[8] M. Kasper, G. Regl, A.M. Frischauf, F. Aberger, GLI transcription factors: mediators of oncogenic Hedgehog signalling, Eur. J. Cancer 42 (2006) 437–445.

[9] T. Osterlund, P. Kogerman, Hedgehog signalling: how to get from Smo to Ci and Gli, Trends Cell Biol. 16 (2006) 176–180.

[10] M. Varjosalo, S.P. Li, J. Taipale, Divergence of hedgehog signal transduction mechanism between Drosophila and mammals, Dev. Cell 10 (2006) 177–186.

[11] J. Briscoe, A. Pierani, T.M. Jessell, J. Ericson, A homeodomain protein code specifies progenitor cell identity and neuronal fate in the ventral neural tube, Cell 101 (2000) 435–445.

[12] R.O. Karlstrom, O.V. Tyurina, A. Kawakami, N. Nishioka, W.S. Talbot, H. Sasaki, A.F. Schier, Genetic analysis of zebrafish gli1 and gli2 reveals divergent requirements for gli genes in vertebrate development, Development 130 (2003) 1549–1564.

[13] B. Guner, R.O. Karlstrom, Cloning of zebrafish nkx6.2 and a comprehensive analysis of the conserved transcriptional response to Hedgehog/Gli signaling in the zebrafish neural tube, MOD, Gene Expr. Patterns 7 (2007) 596–605.

[14] H. Sasaki, C. Hui, M. Nakafuku, H. Kondoh, A binding site for Gli proteins is essential for HNF-3beta floor plate enhancer activity in transgenics and can respond to Shh in vitro, Development 124 (1997) 1313–1322.

[15] K.W. Kinzler, B. Vogelstein, The GLI gene encodes a nuclear protein which binds specific sequences in the human genome, Mol. Cell. Biol. 10 (1990) 634–642.

[16] P.W. Ingham, M. Placzek, Orchestrating ontogenesis: variations on a theme by sonic hedgehog, Nat. Rev., Genet. 7 (2006) 841–850.

[17] M. Brand, C.P. Heisenberg, R.M. Warga, F. Pelegri, R.O. Karlstrom, D. Beuchle, A. Picker, Y.J. Jiang, M. Furutani-Seiki, F.J. van Eeden, M. Granato, P. Haffter, M. Hammerschmidt, D.A. Kane, R.N. Kelsh, M.C. Mullins, J. Odenthal, C. Nusslein-Volhard, Mutations affecting development of the midline and general body shape during zebrafish embryogenesis, Development 123 (1996) 129–142.

[18] R.O. Karlstrom, T. Trowe, S. Klostermann, H. Baier, M. Brand, A.D. Crawford, B. Grunewald, P. Haffter, H. Hoffmann, S.U. Meyer, B.K. Muller, S. Richter, F.J. van Eeden, C. Nusslein−Volhard, F. Bonhoeffer, Zebrafish mutations affecting retinotectal axon pathfinding, Development 123 (1996) 427–438.

[19] W. Chen, S. Burgess, N. Hopkins, Analysis of the zebrafish smoothened mutant reveals conserved and divergent functions of hedgehog activity, Development 128 (2001) 2385–2396.

[20] Z.M. Varga, A. Amores, K.E. Lewis, Y.L. Yan, J.H. Postlethwait, J.S. Eisen, M. Westerfield, Zebrafish smoothened functions in ventral neural tube specification and axon tract formation, Development 128 (2001) 3497–3509.

[21] M.J. Barresi, H.L. Stickney, S.H. Devoto, The zebrafish slow-muscle-omitted gene product is required for Hedgehog signal transduction and the development of slow muscle identity, Development 127 (2000) 2189–2199.

[22] J. Xu, B.P. Srinivas, S.Y. Tay, A. Mak, X. Yu, S.G. Lee, H. Yang, K.R. Govindarajan, B. Leong, G. Bourque, S. Mathavan, S. Roy, Genome-wide expression profiling in the zebrafish embryo identifies target genes regulated by Hedgehog signaling during vertebrate development, Genetics 174 (2006) 735–752.

[23] P.W. Ingham, A.P. McMahon, Hedgehog signaling in animal development: paradigms and principles, Genes Dev. 15 (2001) 3059–3087.

[24] J. Briscoe, L. Sussel, P. Serup, D. Hartigan-O'Connor, T.M. Jessell, J.L. Rubenstein, J. Ericson, Homeobox gene Nkx2.2 and specification of neuronal identity by graded Sonic hedgehog signalling, Nature 398 (1999) 622–627.

[25] J.P. Concordet, K.E. Lewis, J.W. Moore, L.V. Goodrich, R.L. Johnson, M.P. Scott, P.W. Ingham, Spatial regulation of a zebrafish patched homologue reflects the roles of sonic hedgehog and protein kinase A in neural tube and somite patterning, Development 122 (1996) 2835–2846.

[26] H. Bauer, A. Meier, M. Hild, S. Stachel, A. Economides, D. Hazelett, R.M. Harland, M. Hammerschmidt, Follistatin and noggin are excluded from the zebrafish organizer, Dev. Biol. 204 (1998) 488–507.

[27] H. Amthor, B. Christ, F. Rashid−Doubell, C.F. Kemp, E. Lang, K. Patel, Follistatin regulates bone morphogenetic protein−7 (BMP−7) activity to stimulate embryonic muscle growth, Dev. Biol. 243 (2002) 115–127.

[28] A. Fainsod, K. Deissler, R. Yelin, K. Marom, M. Epstein, G. Pillemer, H. Steinbeisser, M. Blum, The dorsalizing and neural inducing gene follistatin is an antagonist of BMP-4, Mech. Dev. 63 (1997) 39–50.

[29] K.F. Liem Jr., T.M. Jessell, J. Briscoe, Regulation of the neural patterning activity of sonic hedgehog by secreted BMP inhibitors expressed by notochord and somites, Development 127 (2000) 4855–4866.

[30] V.P. Gallo, A. Civinini, Survey of the adrenal homolog in teleosts, Int. Rev. Cyt. 230 (2003) 89–187.

[31] T. Else, G.D. Hammer, Genetic analysis of adrenal absence: agenesis and aplasia, Trends Endocrinol. Metab. 16 (2005) 458–468.

[32] F. Bollig, R. Mehringer, B. Perner, C. Hartung, M. Schafer, M. Schartl, J.N. Volff, C. Winkler, C. Englert, Identification and comparative expression analysis of a second wt1 gene in zebrafish, Dev. Dyn. 235 (2006) 554–561.

[33] H.J. Hsu, G. Lin, B.C. Chung, Parallel early development of zebrafish interrenal glands and pronephros: differential control by wt1 and ff1b, Development 130 (2003) 2107–2116.

[34] A.E. Urban, X. Zhou, J.M. Ungos, D.W. Raible, C.R. Altmann, P.D. Vize, FGF is essential for both condensation and mesenchymal–epithelial transition stages of pronephric kidney tubule development, Dev. Biol. 297 (2006) 103–117.

[35] C. Chai, Y.W. Liu, W.K. Chan, Ff1b is required for the development of steroidogenic component of the zebrafish interrenal organ, Dev. Biol. 260 (2003) 226–244.

[36] J. Bose, L. Grotewold, U. Ruther, Pallister–Hall syndrome phenotype in mice mutant for Gli3, Hum. Mol. Genet. 11 (2002) 1129–1135.

[37] F. Cavodeassi, R. Diez Del Corral, S. Campuzano, M. Dominguez, Compartments and organising boundaries in the Drosophila eye: the role of the homeodomain Iroquois proteins, Development 126 (1999) 4933–4942.

[38] J.L. Gomez-Skarmeta, J. Modolell, Araucan and caupolican provide a link between compartment subdivisions and patterning of sensory organs and veins in the Drosophila wing, Genes Dev. 10 (1996) 2935–2945.

[39] J.L. Gomez-Skarmeta, A. Glavic, E. de la Calle-Mustienes, J. Modolell, R. Mayor, Xiro, a Xenopus homolog of the Drosophila Iroquois complex genes, controls development at the neural plate, EMBO J. 17 (1998) 181–190.

[40] C.W. Cheng, C.H. Yan, C.C. Hui, U. Strahle, S.H. Cheng, The homeobox gene irx1a is required for the propagation of the neurogenic waves in the zebrafish retina, Mech. Dev. 123 (2006) 252–263.

[41] X. Wang, A. Emelyanov, I. Sleptsova−Friedrich, V. Korzh, Z. Gong, Expression of two novel zebrafish iroquois homologues (ziro1 and ziro5) during early development of axial structures and central nervous system, Mech. Dev. 105 (2001) 191–195.

[42] M. Furuse, H. Sasaki, K. Fujimoto, S. Tsukita, A single gene product, claudin−1 or −2, reconstitutes tight junction strands and recruits occludin in fibroblasts, J. Cell Biol. 143 (1998) 391–401.

[43] J.M. Bronstein, Function of tetraspan proteins in the myelin sheath, Curr. Opin. Neurobiol. 10 (2000) 552–557.

[44] D.B. Simon, Y. Lu, K.A. Choate, H. Velazquez, E. Al-Sabban, M. Praga, G. Casari, A. Bettinelli, G. Colussi, J. Rodriguez−Soriano, D. McCredie, D. Milford, S. Sanjad, R.P. Lifton, Paracellin-1, a renal tight junction protein required for paracellular Mg^{2+} resorption, Science 285 (1999) 103–106.

[45] E.R. Wilcox, Q.L. Burton, S. Naz, S. Riazuddin, T.N. Smith, B. Ploplis, I. Belyantseva, T. Ben-Yosef, N.A. Liburd, R.J. Morell, B. Kachar, D.K. Wu, A.J. Griffith, T.B. Friedman, Mutations in the gene encoding tight junction claudin-14 cause autosomal recessive deafness DFNB29, Cell 104 (2001) 165–172.

[46] R. Kollmar, S.K. Nakamura, J.A. Kappler, A.J. Hudspeth, Expression and phylogeny of claudins in vertebrate primordia, Proc. Natl. Acad. Sci. U. S. A. 98 (2001) 10196–10201.

[47] V. Korzh, I. Sleptsova, J. Liao, J. He, Z. Gong, Expression of zebrafish bHLH genes ngn1 and nrd defines distinct stages of neural differentiation, Dev. Dyn. 213 (1998) 92–104.

[48] F.J. Naya, H.P. Huang, Y. Qiu, H. Mutoh, F.J. DeMayo, A.B. Leiter, M.J. Tsai, Diabetes, defective pancreatic morphogenesis, and abnormal enteroendocrine differentiation in BETA2/neuroD-deficient mice, Genes Dev. 11 (1997) 2323–2334.

[49] P. Andermann, J. Ungos, D.W. Raible, Neurogenin1 defines zebrafish cranial sensory ganglia precursors, Dev. Biol. 251 (2002) 45–58.

[50] S.A. Koblar, M. Murphy, G.L. Barrett, A. Underhill, P. Gros, P.F. Bartlett, Pax-3 regulates neurogenesis in neural crest-derived precursor cells, J. Neurosci. Res. 56 (1999) 518–530.

[51] S.H. Devoto, W. Stoiber, C.L. Hammond, P. Steinbacher, J.R. Haslett, M.J. Barresi, S.E. Patterson, E.G. Adiarte, S.M. Hughes, Generality of vertebrate developmental patterns: evidence for a dermomyotome in fish, Evol. Dev. 8 (2006) 101–110.

[52] C. Marcelle, S. Ahlgren, M. Bronner-Fraser, In vivo regulation of somite differentiation and proliferation by Sonic Hedgehog, Dev. Biol. 214 (1999) 277–287.

[53] X. Feng, E.G. Adiarte, S.H. Devoto, Hedgehog acts directly on the zebrafish dermomyotome to promote myogenic differentiation, Dev. Biol. 300 (2006) 736–746.

[54] J.T. Eggenschwiler, E. Espinoza, K.V. Anderson, Rab23 is an essential negative regulator of the mouse Sonic hedgehog signalling pathway, Nature 412 (2001) 194–198.

[55] F. Ulloa, N. Itasaki, J. Briscoe, Inhibitory Gli3 activity negatively regulates Wnt/beta-catenin signaling, Curr. Biol. 17 (2007) 545–550.

[56] A. Gulacsi, L. Lillien, Sonic hedgehog and bone morphogenetic protein regulate interneuron development from dorsal telencephalic progenitors in vitro, J. Neurosci. 23 (2003) 9862–9872.

[57] V. Palma, A. Ruiz i Altaba, Hedgehog–GLI signaling regulates the behavior of cells with stem cell properties in the developing neocortex, Development 131 (2004) 337–345.

[58] A. Ruiz i Altaba, B. Stecca, P. Sanchez, Hedgehog–Gli signaling in brain tumors: stem cells and paradevelopmental programs in cancer, Cancer Lett. 204 (2004) 145–157.

[59] M. Westerfield, The Zebrafish Book; A Guide for the Laboratory Use of Zebrafish (*Danio rerio*), 4th ed. Univ. of Oregon Press, Eugene, OR, 2000.

[60] C.B. Kimmel, W.W. Ballard, S.R. Kimmel, B. Ullmann, T.F. Schilling, Stages of embryonic development of the zebrafish, Dev. Dyn. 203 (1995) 253–310.

[61] S.C. Ekker, A.R. Ungar, P. Greenstein, D.P. von Kessler, J.A. Porter, R.T. Moon, P.A. Beachy, Patterning activities of vertebrate hedgehog proteins in the developing eye and brain, Curr. Biol. 5 (1995) 944–955.

[62] C.E. Horak, J.H. Lee, A.G. Elkahloun, M. Boissan, S. Dumont, T.K. Maga, S. Arnaud-Dabernat, D. Palmieri, W.G. Stetler-Stevenson, M.L. Lacombe, P.S. Meltzer, P.S. Steeg, Nm23-H1 suppresses tumor cell motility by down-regulating the lysophosphatidic acid receptor EDG2, Cancer Res. 67 (2007) 7238–7246.

[63] R.O. Karlstrom, W.S. Talbot, A.F. Schier, Comparative synteny cloning of zebrafish you-too: mutations in the Hedgehog target gli2 affect ventral forebrain patterning, Genes Dev. 13 (1999) 388–393.

[64] H.C. Seo, B.O. Saetre, B. Havik, S. Ellingsen, A. Fjose, The zebrafish Pax3 and Pax7 homologues are highly conserved, encode multiple isoforms and show dynamic segment-like expression in the developing brain, Mech. Dev. 70 (1998) 49–63.

[65] F.C. Serluca, M.C. Fishman, Pre-pattern in the pronephric kidney field of zebrafish, Development 128 (2001) 2233–2241.

[66] C. Chai, W.K. Chan, Developmental expression of a novel Ftz-F1 homologue, ff1b (NR5A4), in the zebrafish Danio rerio, Mech. Dev. 91 (2000) 421–426.

[67] V. Lecaudey, I. Anselme, R. Dildrop, U. Ruther, S. Schneider-Maunoury, Expression of the zebrafish Iroquois genes during early nervous system formation and patterning, J. Comp. Neurol. 492 (2005) 289–302.